

this would suggest a more uniform flow downstream; in practical applications, such as hypersonic flow inlets, this would be desirable. Since the flow separation is not eliminated, however, surface heating penalties may outweigh this benefit. Further studies are required to examine the optimization of the surface porosity. This modified Navier-Stokes code may complement future wind-tunnel testing.

Acknowledgments

The author acknowledges the North Carolina Supercomputing Program for providing computational resources on the Cray Y-MP computer. The author wishes to acknowledge the guidance and patience of Ndaona Chokani, and thanks Algacyr Morgenstern for providing a version of his Navier-Stokes code and discussions concerning its use.

References

- Chokani, N., and Squire, L. C., "Transonic Shockwave/Turbulent Boundary Layer Interactions On a Porous Surface," *Aeronautical Journal*, Vol. 97, May 1993, pp. 163-170.
- Rallo, R., "An Investigation of Passive Control Methods for Shock-Induced Separation at Hypersonic Speeds," M.S. Thesis, Univ. of Michigan, 1992.
- Morgenstern, A., and Chokani, N., "Hypersonic Flow Past Open Cavities," *AIAA Journal*, Vol. 32, No. 12, 1994, pp. 2387-2393.
- Kim, J., and Chokani, N., "Navier-Stokes Study of a Supersonic Cavity Flowfield with Passive Control," *Journal of Aircraft*, Vol. 29, No. 2, 1992, pp. 217-223.

Computation of Transonic Flows with Shock-Induced Separation Using Algebraic Turbulence Models

S. K. Chakrabarty* and K. Dhanalakshmi†
National Aerospace Laboratories,
Bangalore 560 017, India

Introduction

CONSIDERABLE advancement in the computation of viscous transonic flows using compressible, Reynolds-averaged, Navier-Stokes equations with turbulence models has been achieved recently due to the availability of high-speed computers and the substantial improvement in the efficiency and accuracy of the numerical algorithms. However, for complex flow situations, such as transonic flow past bodies of aerodynamic interest, more effort is necessary to achieve an efficient and reliable solution. The finite volume method is well known for its capability to handle complex geometrical shapes, and it has reached maturity as far as the accuracy of the solution is concerned provided the flow remains laminar and the computational grid is appropriately generated to suit the complexity of the flow and the geometry. However, for turbulent flows, accuracy of the solution depends largely on the turbulence model used to close the system of governing equations. Over the last 20 years the rate of progress in turbulence modeling has been pretty slow compared with that in the development of high-speed computers which, in turn, has led to an increase in the geometrical and fluid mechanical complexity attainable by simulations. The eddy-viscosity-based turbulence models necessarily produce pseudolaminar solutions with the stresses closely linked to the mean

flow gradients; they may be well behaved but they are not usually very accurate away from the flows for which they have been calibrated. Turbulence models based on term-by-term modeling of the Reynolds-stress transport equations produce solutions which may be accurate in some cases but are liable to fail rather badly in other cases; that is, they are ill behaved in a way that eddy-viscosity methods are not.¹ Algebraic turbulence models²⁻⁴ have been extended by others far beyond the domain intended by their originators because of their simplicity in use and the virtue of almost never breaking down computationally.

Finite volume spatial discretization with Runge-Kutta time stepping scheme developed for the Euler equations has been successfully extended by Swanson and Turkel⁵ to the viscous flow computation using thin-layer Navier-Stokes equations, and similar procedures are being used by many others.^{6,7} These methods follow cell-centered finite volume formulation, where the flow quantities are associated with the center of a cell in the computational mesh and the fluxes across the cell boundaries are calculated using arithmetic means of the values in the adjacent cells. In these schemes the procedure used to compute the pressure on the boundary incorporates the boundary-layer type of approximation, i.e., the zero normal pressure gradient inside the boundary layer. However, in real flows, the normal pressure gradient is not negligible and it may cause confusion in tests of turbulence models.

On the other hand, cell-vertex or nodal point schemes proposed by Ni⁸ and Hall⁹ for Euler equations have been extended to solve Navier-Stokes equations originally presented by Chakrabarty^{10,11} and later used and extended to three dimensions by Radespiel¹² with thin-layer approximation. The main advantages of the vertex-based schemes over cell-centered schemes are 1) the accuracy in the computations of derivatives, particularly for stretched and skewed grids and 2) direct computation of pressure on the wall. A novel vertex-based (nodal point) spatial discretization scheme in the framework of finite volume method has been proposed by Chakrabarty,¹³ which gives second-order accurate first derivatives and at least first-order accurate second derivatives even for stretched and skewed grids. This scheme takes almost the same numerical effort to solve full Reynolds-averaged Navier-Stokes equations as that for thin-layer approximation.

In the present work, the finite volume method based on the nodal point approach introduced earlier in Ref. 13 has been used with algebraic turbulence models proposed by Cebeci and Smith^{2,3} and Baldwin and Lomax.⁴ Further improvements of these basic models proposed by Radespiel¹² and Goldberg¹⁴ for separated flows have been implemented and studied by computing three typical examples having strong shocks with shock-induced separated bubble. The details regarding the governing equations, boundary conditions, finite volume space discretization, the five-stage Runge-Kutta time stepping and the acceleration techniques are available in Ref. 13.

Turbulence Modeling

Algebraic turbulence modeling introduced by Cebeci and Smith^{2,3} and later modified by Baldwin and Lomax⁴ for the outer region, where the necessity to compute the displacement thickness for the eddy length scale was replaced by the local vorticity, works well for attached flows. Transonic flows with strong shocks exhibit a small separation bubble at the foot of the shock. Existing turbulence models either do not treat such bubbles or do so in an ad hoc fashion. Goldberg¹⁴ attempted to address this problem in a rigorous manner and proposed a model to treat the separated region. His model is based on the assumption and observation that 1) the stress scale is given by the maximum shear stress in the separated layer, not by the wall stress as proposed by Baldwin and Lomax and 2) the shear layer has qualitatively the same turbulent structure when it is detached as when it is attached and the length scale is the height of the separated region. Radespiel¹² also used a similar idea by replacing the distance from the wall by the distance from the minimum velocity line (see Fig. 1 for nomenclature) and the shear stress at the wall by its maximum value to prevent vanishing eddy viscosity at the separation point. He, however, did not treat the region between the wall and the minimum velocity line. He obtained a pressure distribution with stronger shock downstream of the experimental

Received Aug. 15, 1994; revision received Dec. 9, 1994; accepted for publication Jan. 20, 1995. Copyright © 1995 by S. K. Chakrabarty and K. Dhanalakshmi. Published by the American Institute of Aeronautics and Astronautics, Inc., with permission.

*Scientist, Computational and Theoretical Fluid Dynamics Division. Senior Member AIAA.

†Scientist, Computational and Theoretical Fluid Dynamics Division.

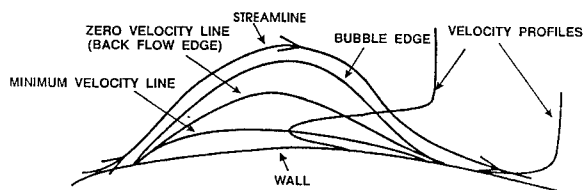


Fig. 1 Schematic view of separated flow bubble and its nomenclature.

shock position and skin-friction distribution shows separation but no reattachment on the aerofoil. However, by using the Johnson and King¹⁵ model, which is not simply an eddy-viscosity model but also contains features of a Reynolds stress model, the results improved both in shock position and skin-friction distribution with reattachment near the trailing edge. The aftershock comparison still has scope for improvement. It has been also observed by others⁷ that the Baldwin and Lomax model predicts shock position downstream of that observed in experiment. We have studied various possibilities, models 1–4. In model 1 the turbulent inner viscosity has been calculated by the Cebeci and Smith model²; turbulent outer viscosity for the body and the wake has been calculated by the Baldwin and Lomax model¹⁴; for the separated region, normal distance from the wall has been replaced by normal distance from the minimum velocity line inside the bubble; and between the wall and the minimum velocity line, the normal distance has been replaced by the minimum of the two distances measured from the wall and from the minimum velocity line. The shear stress at the wall has been replaced by its maximum over a normal direction grid line inside the bubble. Model 2 is the same as model 1 with turbulent inner viscosity also calculated by Baldwin and Lomax with the modification for normal distance and the wall shear stress. Model 3 is the same as model 1 with a change in the treatment inside the bubble (back flow region) as suggested by Goldberg,¹⁴ and model 4 is the same as model 2 with similar change inside the bubble as suggested by Goldberg.

Results and Discussion

Three examples are considered here, and for all three a C type algebraic grid (257×61) where minimum normal spacing of 10^{-5} with chord length as unity has been used such that the maximum y^+ value at the first grid node is of the order of four. Far-field boundary of the computational domain has been placed about 10 chords away from the aerofoil.

For the first example, pressure coefficient C_P distributions on the aerofoil and skin-friction coefficient C_f distributions on the upper surface for a RAE-2822 aerofoil at a free-stream Mach number $M_\infty = 0.75$, angle of attack $\alpha = 2.81$ deg, and Reynolds number $Re_\infty = 6.2 \times 10^6$ obtained by using the four models are shown in Fig. 2 along with the experimental results.¹⁶ In the models computed shock is stronger, its position is downstream of that observed by experiment, and higher pressure has been predicted in the post-shock region. All of the four models have predicted almost identical pressure distributions. Skin-friction distributions compare well with experiment, and the separated region at the foot of the shock has been clearly predicted. Models 1 and 2 have shown identical C_f distribution, but models 3 and 4 have predicted slightly longer separation bubble.

For the NACA 0012 aerofoil at $M_\infty = 0.799$, $\alpha = 2.26$ deg, and $Re_\infty = 9.0 \times 10^6$, surface C_P distributions and uppersurface C_f distributions are shown in Fig. 3 along with the experimental C_P distribution.¹⁷ In this case, too, predicted shock is stronger and its position is downstream of that observed in experiments. C_P distributions at the foot of the shock obtained by models 3 and 4 differ from those obtained by models 1 and 2, and C_f distributions show similar differences as in the first example case.

The third example considered is transonic flow past a CAST-7 aerofoil at $M_\infty = 0.7$, $\alpha = 4.59$ deg, and $Re_\infty = 5.96 \times 10^6$. This case was studied by Johnston,⁷ and he used one-equation turbulence model. His computation predicted stronger shock and large differences in shock position and downstream pressure levels with respect to the experimental results.¹⁸ Present computation also shows similar results. Computed C_P distributions and uppersurface C_f distributions are shown in Fig. 4 along with the exper-

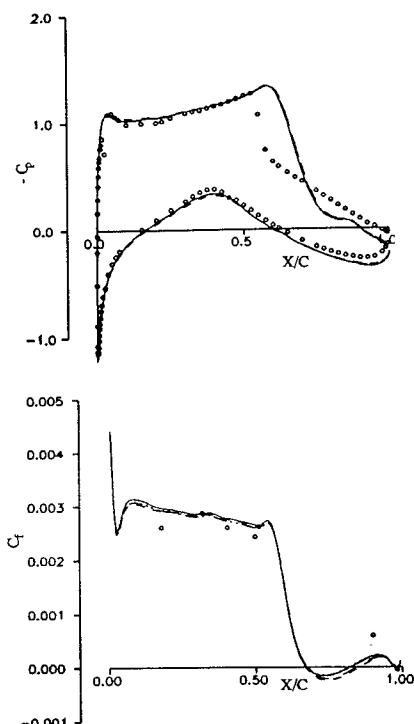


Fig. 2 Surface pressure and skin friction distributions for RAE-2822 aerofoil, $M_\infty = 0.75$, $\alpha = 2.81$ deg, $Re_\infty = 6.2 \times 10^6$, grid 257×61 : —, model 1; ·····, model 2; - - - -, model 3; - - -, model 4; ○ ○ ○, experiment.

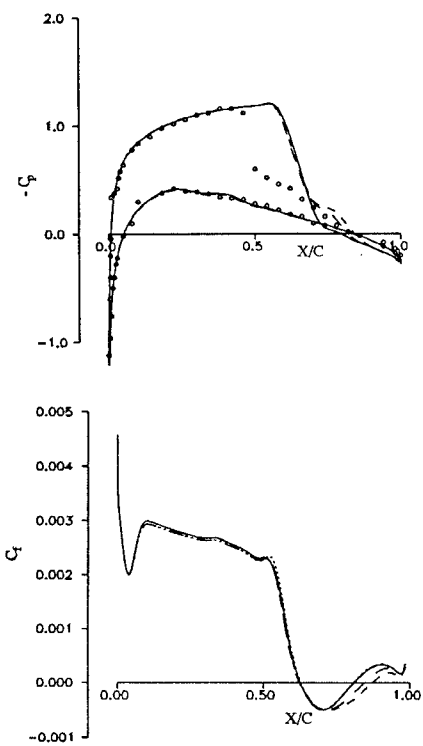


Fig. 3 Surface pressure and skin friction distributions for NACA-0012 aerofoil, $M_\infty = 0.799$, $\alpha = 2.26$ deg, $Re_\infty = 9.0 \times 10^6$, grid 257×61 : —, model 1; ·····, model 2; - - - -, model 3; - - -, model 4; ○ ○ ○, experiment.

imental C_P distribution.¹⁸ As in the previous two cases, the four models predicted almost same pressure and skin-friction distribution with stronger shock located downstream of the experimental position. Shock-induced separation predicted over the region $0.48 < x/c < 0.60$ by all of the models compares well with that ($0.51 < x/c < 0.59$) predicted in Ref. 7. Position of the separation point at the foot of the shock indicates the present shock position is closer to experiment than obtained in Ref. 7.

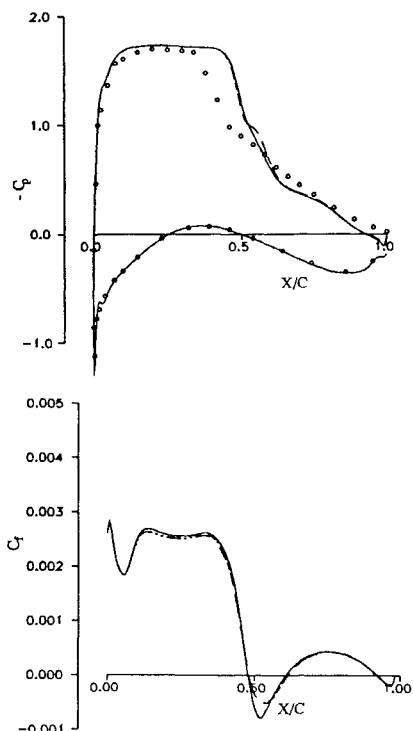


Fig. 4 Surface pressure and skin friction distributions for CAST-7 aerofoil, $M_\infty = 0.70$, $\alpha = 4.59$ deg, $Re_\infty = 5.96 \times 10^6$, grid 257×61 : —, model 1; ···, model 2; - - -, model 3; - - -, model 4; ○○○○, experiment.

For the three cases computed here, all of the four models predicted the separation point at approximately the same location. Reattachment points are same for models 1 and 2 but differ a little for models 3 and 4 in the first two cases. In the third case all of the models predicted the same separation and reattachment points. An overall good C_f distribution has been obtained by all of the four models. The basic criteria to compute shock-induced separated flows are the replacement of the wall shear stress by its local maximum value inside the bubble, and the replacement of the normal distance from the wall by the normal distance from the minimum velocity line in models 1 and 2 and from the back flow edge in models 3 and 4. Fine grid (495×91) computation (results not shown here) also showed similar behavior. This study also suggests that the flow between the wall and the minimum velocity line inside the bubble can be treated as laminar, and outside the minimum velocity line the flow behaves like attached flow.

We infer from this analysis that algebraic turbulence models, in general, predict stronger shock, but the separation bubble at the foot of the shock and the skin-friction distribution can be predicted well by any of the four models described earlier. As pointed out by Bradshaw,¹ for transonic flows, the normal pressure gradient is not negligible inside the boundary-layer and so does not obey the boundary-layer assumption. In the present algorithm this assumption has been used only through the turbulence model. The velocity gradient produced due to this, in principle, leads to extra production of turbulence through the product of mean velocity gradient and turbulent shear stress. Prediction of correct wall shear stress by the present models merely implies correct prediction of mean velocity profiles and not the velocity gradients. In rapidly growing flows near separation, where normal pressure gradients affect the mean velocity gradient, one cannot expect an acceptable pressure distribution. So, for better results in both skin friction and pressure distribution, turbulence models should be developed for Navier-Stokes computations without any boundary-layer type of approximations.

References

- Bradshaw, P., "Turbulence: The Chief Outstanding Difficulty of Our Subject," *Experiments in Fluids*, Vol. 16, No. 2, 1994, pp. 203-216.
- Cebeci, T., Smith, A. M. O., and Mosinski, G., "Calculation of Compressible Adiabatic Turbulent Boundary Layers," *AIAA Journal*, Vol. 8, No. 11, 1970, pp. 1974-1982.
- Cebeci, T., and Smith, A. M. O., "Analysis of Turbulent Boundary Layers," *Applied Mathematics and Mechanics*, Academic, New York, 1974.
- Baldwin, B. S., and Lomax, H., "Thin Layer Approximation and Algebraic Model for Separated Turbulent Flows," *AIAA Paper 78-257*, Jan. 1978.
- Swanson, R. C., and Turkel, E., "A Multistage Time Stepping Scheme for the Navier-Stokes Equations," *AIAA Paper 85-0035*, Jan. 1985.
- Müller, B., and Rizzi, A., "Runge-Kutta Finite Volume Simulation of Laminar Transonic Flow over a NACA-0012 Airfoil Using the Navier-Stokes Equations," *Aeronautical Research Inst. of Sweden, FFA TN 1986-60*, Stockholm, Sweden, Nov. 1986.
- Johnston, L. J., "Solution of the Reynolds-averaged Navier-Stokes Equations for Transonic Airfoil Flows," *Aeronautical Journal*, Vol. 95, No. 948, 1991, pp. 253-273.
- Ni, R. H., "A Multiple Grid Scheme for Solving the Euler Equations," *AIAA Journal*, Vol. 20, No. 11, 1992, pp. 1565-1571.
- Hall, M. G., "Cell Vertex Multigrid Scheme for Solution of Euler Equations," *RAE-TM-Aero-2029*, March 1985.
- Chakrabarty, S. K., "Numerical Solution of Navier-Stokes Equations for Two-Dimensional Viscous Compressible Flows," *AIAA Journal*, Vol. 27, No. 7, 1989, pp. 843, 844.
- Chakrabarty, S. K., "Vertex Based Finite Volume Solution of the Two-Dimensional Navier-Stokes Equations," *AIAA Journal*, Vol. 28, No. 10, 1990, pp. 1829-1831.
- Radespiel, R., "A Cell Vertex Multigrid Method for the Navier-Stokes Equations," *NASA TM 101557*, Jan. 1989.
- Chakrabarty, S. K., "A Finite Volume Nodal Point Scheme for Solving Two Dimensional Navier-Stokes Equations," *Acta Mechanica*, Vol. 84, No. 1-2, 1990, pp. 139-153.
- Goldberg, U. C., "Separated Flow Treatment with a New Turbulence Model," *AIAA Journal*, Vol. 24, No. 10, 1986, pp. 1711-1713.
- Johnson, D. A., and King, L. S., "A New Turbulence Closure Model for Boundary Layer Flows with Strong Adverse Pressure Gradients and Separation," *AIAA Paper 84-0175*, Jan. 1984.
- Cook, P. H., McDonald, M. A., and Firmin, M. C. P., "Aerofoil RAE-2822—Pressure Distributions and Boundary Layer and Wake Measurements," *AGARD-AR-138*, May 1979, pp. A6-1-A6-77.
- Harris, C. D., "Two Dimensional Aerodynamic Characteristics of the NACA 0012 Airfoil in the Langley 8-foot Transonic Pressure Tunnel," *NASA TM 81927*, April 1981.
- Stanewsky, E., Puffert, W., Müller, R., and Bateman, T. E. B., "Supercritical Aerofoil CAST-7 Surface Pressure, Wake and Boundary Layer Measurements," *AGARD-AR-138*, May 1979, pp. A3-1-A3-35.

Determination of Starting Shock Velocity in Supersonic Wind Tunnel

Peter J. Disimile*

University of Cincinnati, Cincinnati, Ohio 45221

and

Norman Toy†

University of Surrey,
Guildford GU2 5XH, England, United Kingdom

Introduction

IN the case of many high-speed facilities, the nominal experimental run time is often on the order of seconds or minutes before the facility air is exhausted. During this time the tunnel parameters have to stabilize before measurements are taken, and it is this time period that is very important to the tunnel operating conditions. For supersonic/hypersonic tunnels this time period is related

Received July 29, 1994; revision received Jan 6, 1995; accepted for publication Jan. 6, 1995. Copyright © 1995 by Peter J. Disimile and Norman Toy. Published by the American Institute of Aeronautics and Astronautics, Inc., with permission.

*Bradley Jones Associate Professor, Department of Aerospace Engineering and Engineering Mechanics. Member AIAA.

†Professor in Fluid Mechanics, Department of Civil Engineering.